Total-energy study of electronic structure and mechanical behavior of $C15$ Laves phase compounds: $NbCr_2$ and HfV_2

Alim Ormeci
Theoretical Division, Los Alamos National Laboratory, Los Alamos, New Mexico 87545

F. Chu
Materials Science and Technology Division, Los Alamos National Laboratory, Los Alamos, New Mexico 87545

John M. Wills
Theoretical Division, Los Alamos National Laboratory, Los Alamos, New Mexico 87545

T. E. Mitchell
Materials Science and Technology Division, Los Alamos National Laboratory, Los Alamos, New Mexico 87545

R. C. Albers
Theoretical Division, Los Alamos National Laboratory, Los Alamos, New Mexico 87545

D. J. Thoma
Materials Science and Technology Division, Los Alamos National Laboratory, Los Alamos, New Mexico 87545

S. P. Chen
Theoretical Division, Los Alamos National Laboratory, Los Alamos, New Mexico 87545
(Received 7 May 1996; revised manuscript received 12 July 1996)

First-principles electronic structure calculations based on a full-potential linear muffin-tin orbital method have been used to study the electronic and mechanical properties of the early transition metal $C15$ Laves phase compounds $NbCr_2$ and HfV_2. For both compounds, total energies are computed and compared for the two Laves phase crystal structures $C15$ and $C14$. The lower total-energy structure for $NbCr_2$ is found to be the $C15$ structure as opposed to the $C14$ structure for HfV_2. We have calculated the equilibrium unit cell volumes, bulk moduli, cohesive energies, and heats of formation. We have obtained the density of states and charge density contour plots. Based on these results, we discuss the elastic properties, the stability of the $C15$ phase, and the bonding and deformation mechanisms in Laves phases. [S0163-1829(96)01941-8]

I. INTRODUCTION

Because of the growing interest in intermetallic compounds as potential high-temperature structural materials, there have been many investigations carried out on various compounds,[1] mostly structures that are ordered forms of simple fcc, bcc, and hcp metals. If new intermetallic-based alloys are to be selected on the basis of low density and high melting temperature, as would be required for use in rotating components in the hot sections of gas turbines, for example, then three groups of materials emerge as promising candidates: aluminides,[2] topologically close-packed (TCP) compounds,[3] and silicide-based compounds.[4] In the group of TCP compounds the structure is primarily determined by the ratio of the atomic sizes of the two components such that they can most efficiently fill space.[5] Such structures generally are complex, in that the unit cell contains many atoms, even though the crystal structures may have high symmetry.[5] A number of these compounds have quite high melting temperatures, low densities, and high oxidation resistance, the properties necessary for high-temperature structural applications. However, all three groups of materials have one common disadvantage: They are often brittle at low-temperatures, up to temperatures of hundreds of degrees Celsius. This low-temperature brittleness adversely affects the fabrication and use of these materials. Consequently, it is highly desirable to find ways to improve the low-temperature ductility without compromising much on the attractive high-temperature properties.

The largest subset of TCP intermetallic compounds is the group of Laves phases. In Laves phase systems, a promising approach to enhance ductility at low-temperatures is the addition of a third metal to form a ternary alloy.[6] However, since there are many Laves phase materials, the possibilities of forming ternary alloys for this purpose are countless. A good understanding of the basic properties of binary Laves phase materials will help materials scientists focus on a limited number of systems instead of manufacturing and testing every possible candidate.

Laves phases have either the cubic $C15$ ($MgCu_2$), hexagonal $C14$ ($MgZn_2$), or hexagonal $C36$ ($MgNi_2$) structure.[5] Generally speaking, they have high melting temperatures and fairly low densities.[7] Among the three Laves phase structures, $C15$ Laves phases are expected to show better deformability than the other two Laves phases because of their fcc-based structure (since in the fcc structure more

 © 1996 The American Physical Society

slip systems are available). In the past few years, this expectation has resulted in numerous experimental studies on various $C15$ compounds, for example, $NbCr_2$,[8,9] HfV_2 + Nb,[6,10] $HfCr_2$,[11] $ZrFe_2$[12] and $TiCr_2$.[13] Of these materials, $NbCr_2$ and HfV_2 + Nb, especially, appear to be more promising. $NbCr_2$ has a high melting temperature (1730 °C), reasonable oxidation resistance, high strength, and relatively large range of solubility.[9] $C15$ phase ternary alloys based on the HfV_2 + Nb system also exhibit high melting temperature (1500 °C), high strength, and more importantly improved low-temperature ductility[6,10] compared to the binary $C15$ phase alloys. These experimental findings also make these two materials of theoretical interest. A total energy study of these Laves phase materials will provide general information on their electronic and mechanical properties which will enable us to understand fundamental mechanisms responsible for the observed low- and high-temperature properties. Such an understanding may, then, suggest various criteria or strategies that can be used to improve the low-temperature ductility. A first step toward this goal is to study the structural stability and ground-state properties.

During the last two decades, there have been various first-principles calculations on some $C15$ compounds, mainly to study magnetism and superconductivity, e.g., ZrV_2,[14] $MgZn_2$,[15] $ZrZn_2$,[16] $LaAl_2$, $LuAl_2$, and YAl_2,[17] AFe_2 (A=Sc,Ti,V,Y,Zr,Nb,Lu,Hf,Ta),[18] and AB_2 (A=IIIA-VA transition metal elements, B=VIA-VIIIA transition metal elements).[19] Some simpler calculational methods were used to study the structural stability of Laves phases, e.g., a model potential (pseudopotential) method to investigate the structural stability of $C14$ $MgZn_2$,[20] tight-binding d-bond models to investigate transition metal Laves phase stability among three competing phases ($C15$, $C14$, and $C36$),[21,22] extended Huckel band calculations on model AB_2 compounds to study the relative stability of $C14$ and $C15$ phases,[23] and a more realistic tight-binding method to examine the relationship between the three Laves phases in the Ti-V and Ti-Cr systems.[24] More recently, for $C15$ $NbCr_2$ and HfV_2, the linear muffin-tin orbital method within the atomic sphere approximation (LMTO ASA) has been used to study the equilibrium unit cell volumes, bulk moduli, and electronic properties.[25,26]

In this paper, we present the results of first-principles, all-electron, full-potential, linear muffin-tin orbital (LMTO) based total-energy calculations for $C15$ and $C14$ phase $NbCr_2$ and HfV_2. We have computed various ground-state quantities, and obtained the structural energy differences between the $C15$ and $C14$ phases. We use these results to explain some of the experimental observations, such as phase stability and general trends in high-temperature properties, and also to understand the electronic structure and bonding mechanisms.

This paper is organized as follows. In Sec. II, we briefly describe the $C14$ and $C15$ crystal structures, emphasizing the stacking sequence differences. In Sec. III, details of the calculational method are described. Results are presented in Sec. IV, and their implications are discussed in Sec. V. Conclusions are drawn in Sec. VI.

II. C15 AND C14 CRYSTAL STRUCTURES

The $C15$ structure is face-centered cubic with eight AB_2 formula units per unit cell.[27] It belongs to the space group $Fd3m$-O_h^7, No. 227 in the International Tables. In the primitive unit cell there are six atoms. The $C14$ structure is hexagonal with four AB_2 formula units per cell.[27] It belongs to the space group $P6_3/mmc$-D_{6h}^4, No. 194 in the International Tables. In the primitive unit cell there are 12 atoms. There are two internal degrees of freedom in the atomic positions in the primitive unit cell, and for simplicity we have used the ideal structure values for them.[28]

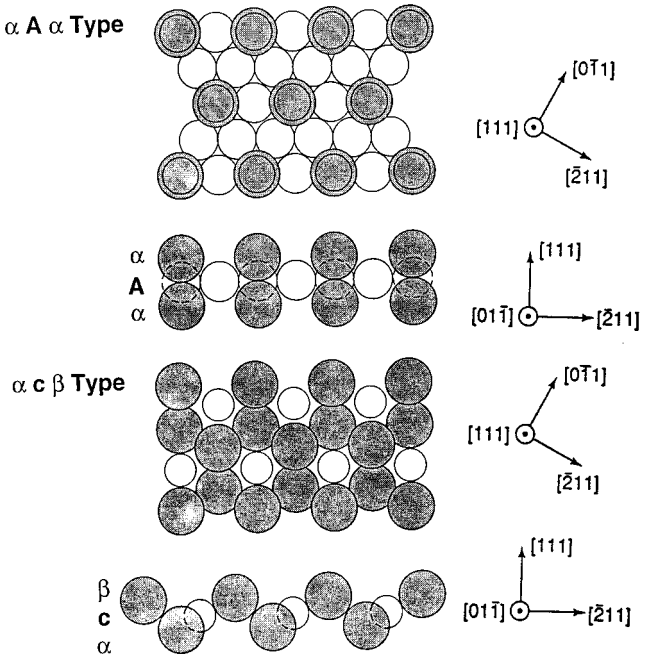

FIG. 1. Two types of sandwich in $C15$ and $C14$ stackings.

The $C15$ and $C14$ structures may be considered as two different kinds of stacking sequences (a third kind giving the other Laves phase structure $C36$). For a Laves phase material AB_2, if we let Greek letters (α, β, γ) denote the A atom planes, lowercase Latin letters (a, b, c) the type-1 B atoms, and capital Latin letters (A, B, C) the type-2 B atoms, then we have the following stacking sequences:[6,11,20]

$$C15\text{: } \ldots\ \ldots\ \alpha A \alpha c \beta B \beta a \gamma C \gamma b\ \ldots\ \ldots,$$

$$C14\text{: } \ldots\ \ldots\ \alpha A \alpha c \beta B \beta c\ \ldots\ \ldots$$

A special structure is characterized by noting the positions of the capital Latin letters, called *Kagomé* nets.[20] Thus, $C15$ is basically ABC stacking and $C14$ is AB stacking. The cubic $C15$ and hexagonal $C14$ structures are related in the same way as fcc and hcp structures.[20] Therefore the Laves phase structures may be described in terms of hexagonal lattices, in which the atomic arrangement leads to values of axial ratios in the proportions 2:3:4 for $C14$:$C15$:$C36$ ($C36$ is $ABAC$ stacking).

In these stacking sequences we can identify two types of sandwiches: (a) α A α (β B β, γ C γ) and (b) α c β (β a γ, γ b α) (see Fig. 1). The packing in these sandwiches and the interlayer distances are quite different as indicated in Fig. 1. The $\alpha A \alpha$ type sandwiches are more widely spaced in the [111] direction and appear to be difficult to shear, presumably due to the directional bonding between the larger

TABLE I. Calculated ground-state quantities for the $C15$ structure. Bulk modulus results are presented both at the theoretical volume (the volume that gives the minimum total energy) and at the experimental volume. Also listed are the experimentally measured bulk modulus values.

Material	Cohesive energy per atom (eV)	Bulk modulus (GPa) At th. vol.	At expt. vol.	Experiment	Deviation from the experimental vol.
$NbCr_2$	6.08	259	191	229.4 [a]	− 6.82%
HfV_2	5.69	171	107	104.0 [b]	−10.75%

[a]Ref. 26.
[b]Ref. 39.

atoms along [111] according to conventional theories. Experimentally, stacking faults have not been observed between these layers.[29] The $\alpha c \beta$-type sandwiches are closely spaced in the [111] direction and also easier to shear, basically due to a shorter shear vector and the possible operation of the synchro-shear mechanism;[6,10,11] correspondingly stacking faults have been observed between these layers in transmission electron microscopy studies.[29]

III. CALCULATIONAL METHOD

We performed total-energy calculations for two intermetallic materials $NbCr_2$ and HfV_2, for the two Laves phase structures $C15$ and $C14$. From these calculations we computed cohesive energies, bulk moduli, heats of formation, and the structural energy differences between the $C15$ and $C14$ phases.

These calculations were carried out with a full-potential, all-electron, electronic-structure method that uses a linear muffin-tin orbital basis set.[30] Basis functions, electron densities, and potentials were expanded in spherical harmonics through $l=6$ within nonoverlapping muffin-tin spheres, and in Fourier series in the interstitial region. The calculations were scalar relativistic and used the Hedin-Lundqvist[31] form of the local density approximation (LDA) exchange-correlation functional with random phase approximation (RPA) parameters.[32] However, an accurate calculation of the heats of formation required the inclusion of spin-orbit coupling, and consequently we carried out fully relativistic calculations for bcc Cr, V, and Nb, hcp Hf, and $C15$ $NbCr_2$ and HfV_2 to compute the heats of formation for the $C15$ structures. The inclusion of spin-orbit coupling does not affect the results pertaining to the structural properties. We have not looked for magnetism in either compound. There are no studies indicating magnetic effects in HfV_2, and previous calculations for $NbCr_2$ using the atomic sphere approximation found the paramagnetic $C15$ phase lower in energy for all relevant volumes than the antiferromagnetic $C15$ phase.[19] Brillouin zone integrations were performed with Fourier quadrature[33] with Gaussian smearing. Calculations for $NbCr_2$ used 23 and 8 irreducible points, with convergence tested to 60 and 35 points, in the $C15$ and $C14$ Brillouin zones, respectively. Calculations for HfV_2 used, respectively, 38 and 17 irreducible points, with convergence tested to 88 and 35 points, in the $C15$ and $C14$ Brillouin zones. The basis set used $2\times(3s,3p)+3\times(4s,4p)+2\times(3d)$ orbitals on each V and Cr site; i.e., vanadium $3s$ orbitals with two different interstitial kinetic energies were included in the basis set. Each Nb site contributed $2\times(4s,4p)+3\times(5s,5p)+2\times(4d)$ orbitals, and each Hf site contributed $2\times(5s,5p)+2\times(6s,6p)+2\times(5d)$ orbitals. A total of three interstitial kinetic energies were used. All basis functions for each calculation were contained in a single, fully hybridized Hamiltonian matrix.

One of the important empirical quantities defined for the Laves phase materials is the ratio of the atomic radii of the two elements. Assuming hard spheres, one obtains $\sqrt{3/2}\sim 1.225$ as the ideal atomic radius ratio of A to B atoms. Although in the full-potential LMTO method one ascribes a muffin-tin sphere to each atom, this sphere is conceptually different from the ''atomic sphere'' mentioned above. Actually, in the full-potential method, the muffin-tin radius is a variational parameter. Therefore, for each material, at their experimental volumes, and for the $C15$ structure only, we performed a number of total-energy calculations by using different muffin-tin radius ratios. The minimization of the total energy gave a muffin-tin radius ratio of 1.12 and 1.02 for $NbCr_2$ and HfV_2, respectively. For all the results presented in this paper, the muffin-tin radii used were determined from these total-energy-minimizing ratios. In both $C14$ and $C15$ calculations, for the same material, the ratio of the total muffin-tin volume to the unit cell volume was kept the same to facilitate a meaningful comparison of total energies.

Finally, for the $C14$ $NbCr_2$ structure we used the experimental c/a ratio, which is equal to 1.6336.[9] Since there is no experimentally observed $C14$ phase for HfV_2, we used the c/a ratio of the $C14$ $NbCr_2$. We did not attempt to minimize the total energy by varying the c/a ratio for either material, since we have found that the $C14$ total energy does not change significantly by varying the c/a ratio (less than 5 meV/atom).

IV. RESULTS

For both materials investigated in this study, the $C15$ structure is the experimentally observed room temperature structure.[9,34] In the phase diagram of $NbCr_2$, there is a structural phase transition from the $C15$ phase to the $C14$ phase at 1585 °C upon heating.[9] For HfV_2, there is no observed $C14$ phase.[34] However, to provide a means of comparison, the calculated values of various ground-state quantities for the $C14$ structures will be listed as well.

We present our results pertaining to the ground-state properties of the $C15$ phase in Table I. The deviation of the calculated equilibrium volume from the experimentally measured one for $NbCr_2$,[9] −6.82%, is well within the usual local density approximation errors. The relatively high contraction

TABLE II. Calculated ground-state quantities for the $C14$ structure. Bulk modulus results are presented both at the theoretical volume (the volume that gives the minimum total energy) and at the volume V'_{expt}. The quantity V'_{expt} is explained in text.

Material	Cohesive energy per atom (eV)	Bulk modulus (GPa)		Deviation from the Volume V'_{expt}
		At theoretical vol.	At volume V'_{expt}	
$NbCr_2$	6.06	256	192	− 6.67%
HfV_2	5.71	173	113	−10.64%

of the volume,[6] 10.75%, for the case of HfV_2 may be reminiscent of the fact that full-potential methods based on the LDA give a value which is off by about 10% for the volume of elemental V.[35] The LMTO-ASA method is a more approximate approach than the full-potential LDA calculations. It is fortuitous that the equilibrium volumes calculated for these materials by the LMTO-ASA method[25,26] are so close to the experimental values.

The corresponding $C14$ phase results are summarized in Table II. Due to the fact that the number of atoms in the primitive unit cell of $C14$ is twice that of $C15$, and that $C14$ is not the observed ground-state structure, we define a volume V'_{expt}, as $V'_{expt}=2\times V_{C15\,expt}$, and use it as the reference volume for $C14$ phase analyses. Here, the quantity, $V_{C15\,expt}$, refers to the experimentally measured volume of the $C15$ structure.

The volume dependence of the total energy is shown in Figs. 2 and 3 for $NbCr_2$ and HfV_2, respectively. We used a fourth-order Birch-Murnaghan equation of state[36] to fit the total energies. We see from Fig. 2 that the $C15$ phase $NbCr_2$ is correctly placed as the lower-energy phase compared to the $C14$ phase throughout the whole range of unit cell volumes. On the other hand, Fig. 3 shows that the $C15$ phase HfV_2 has a higher total energy than the $C14$ phase HfV_2. This suggests that the $C15$ phase is not the low-temperature structure. So, in theory, one expects to observe a $C15 \rightarrow C14$ phase transformation at some lower-temperature. However, it is likely that the transformation temperature is so low that the diffusion rates are too sluggish and the compound stays in the $C15$ structure.

We computed the density of states for $C15$ $NbCr_2$ and HfV_2 at the experimental volume. Figures 4 and 5 show the total and partial density of states for $NbCr_2$ and HfV_2, respectively. The Fermi level of $NbCr_2$ crosses the density of states curve quite close to a small local maximum, whereas that of HfV_2 crosses at a relatively high local minimum. The density of states at the Fermi energy, $N(E_F)$, is found to be 115.8 and 197.9 states/Ry/unit cell for $NbCr_2$ and HfV_2, respectively. For both materials, the density of states near the Fermi level is dominated by the d states [cf. panels (b) and (c) of Figs. 4 and 5]. If we represent the binary $C15$ compound as AB_2, then we also observe that the most dominant contribution comes from the d states of the B atoms. In the case of HfV_2, the contribution of the V d states is 140 states/Ry/unit cell compared to 28.0 states/Ry/unit cell for Hf d

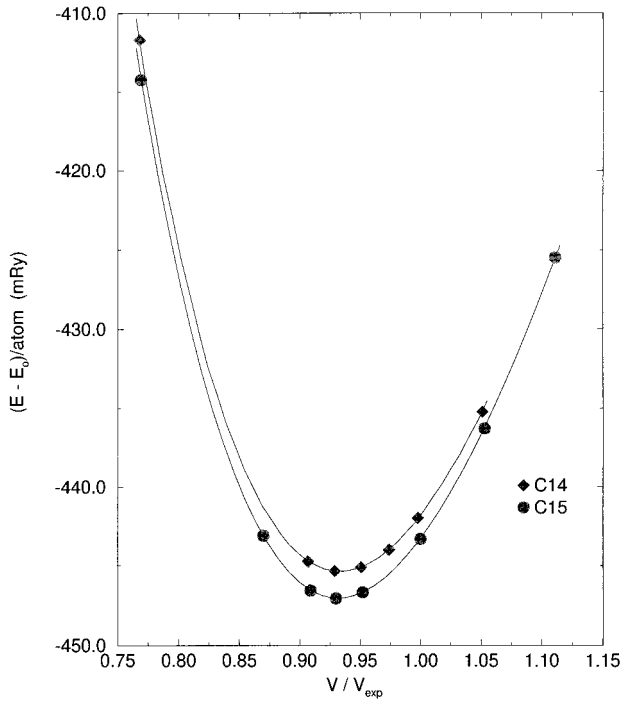

FIG. 2. Cohesive energy per atom plotted as a function of the normalized volume for both $C15$ and $C14$ $NbCr_2$.

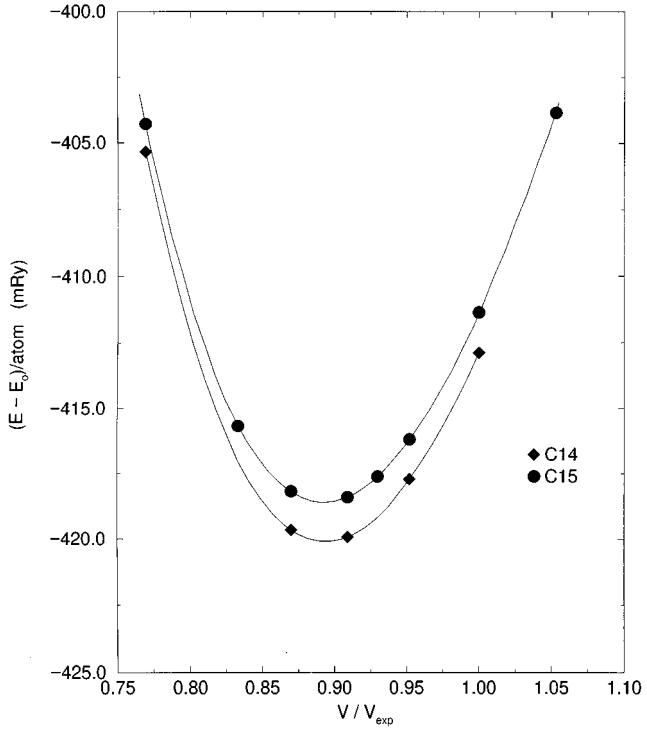

FIG. 3. Cohesive energy per atom plotted as a function of the normalized volume for both $C15$ and $C14$ HfV_2.

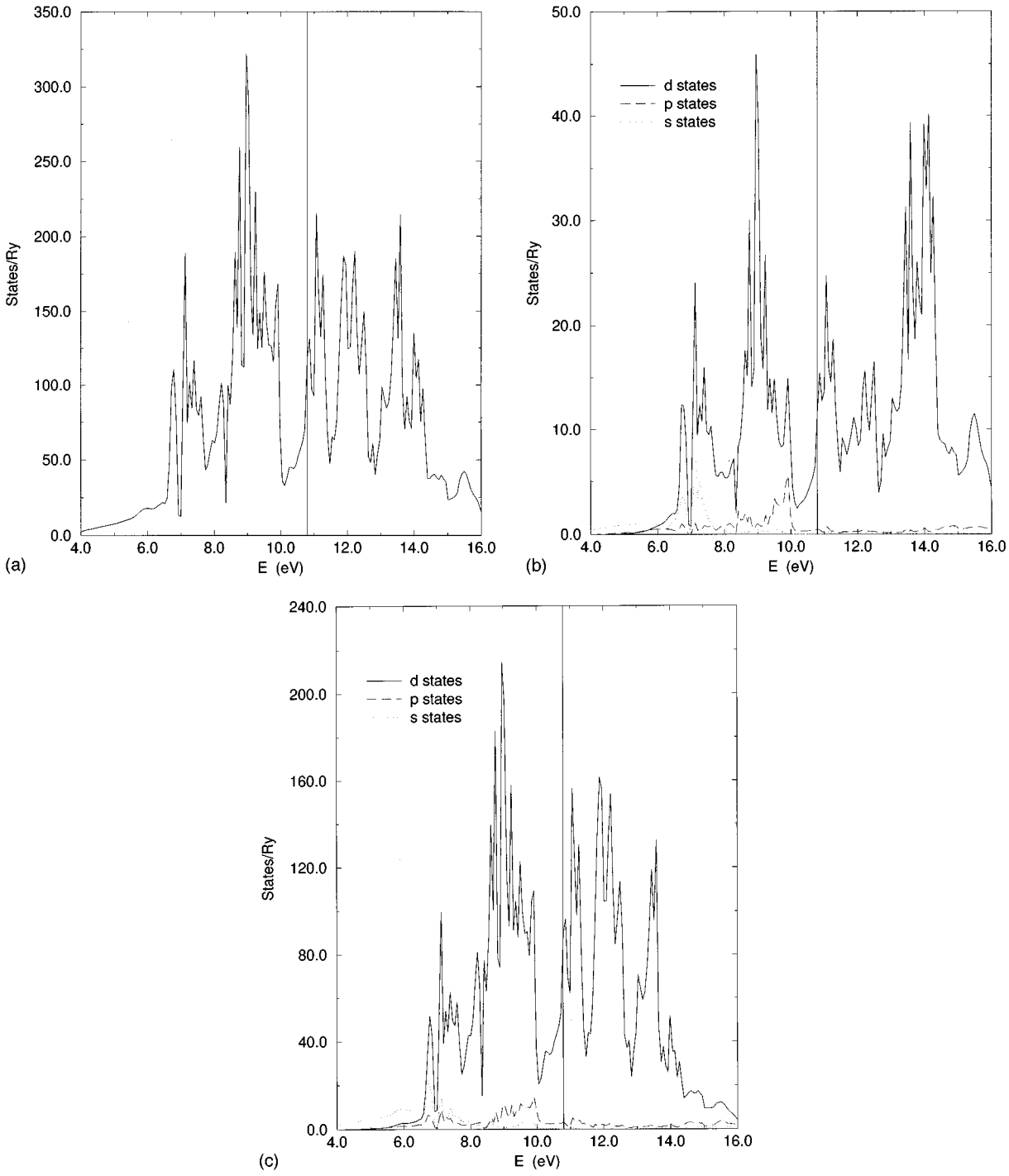

FIG. 4. (a) Total density of states for $C15$ $NbCr_2$, (b) partial density of states for Nb, and (c) partial density of states for Cr.

states. For $NbCr_2$, Cr d and Nb d contributions are 89.0 and 23.6 states/Ry/unit cell, respectively. We also notice one difference between HfV_2 and $NbCr_2$ regarding the contributions of the B atom p states to $N(E_F)$. While the V p contribution to $N(E_F)$ is of the order of that of the Hf d states, 22.0 states/Ry/unit cell, the contribution of the Cr p states is not significant, about 3.2 states/Ry/unit cell, compared with the Nb d states. These full-potential results are in agreement with the LMTO-ASA results.[25,26]

We have also generated charge density contour plots. The (110) bulk plane of the $C15$ structure is chosen since it contains the [111] direction and the two different Laves phase sandwiches discussed earlier. These plots give us some idea about the bonding characteristics. The positions of the atoms lying on this plane are shown in Fig. 6. The contour plots that we obtained are presented in Figs. 7 and 8 for $C15$ $NbCr_2$ and HfV_2, respectively. As discussed in the next section, they show that the bonding is only weakly directional.

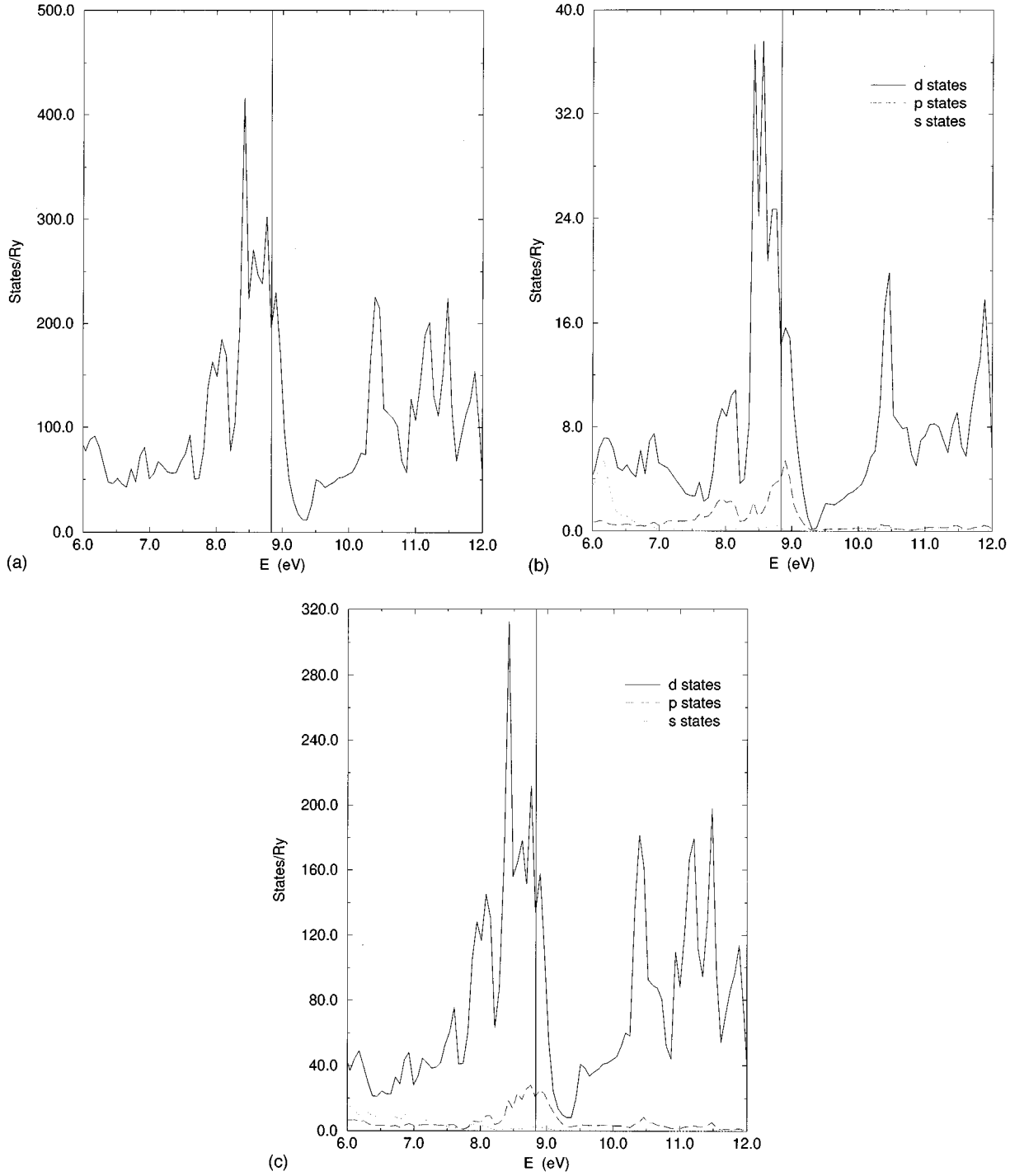

FIG. 5. (a) Total density of states for $C15$ HfV_2, (b) partial density of states for Hf, and (c) partial density of states for V.

V. DISCUSSION

A. Cohesive energies

First-principles calculations can be used to obtain information which may be difficult to obtain by experimental methods. For example, in the case of Laves phase materials, cohesive energy and heat of formation measurements are not widely available. Most of the theoretical methods which are used to study defects, deformation mechanisms, grain boundaries, etc., rely on empirical interatomic potentials whose determination requires cohesive energy as one of the quantities in the fitting procedure.[37]

For Laves phases, as is generally true for most metals and other intermetallic compounds, the higher the melting temperature, the larger the cohesive energy. Although experimental values for the cohesive energies of $NbCr_2$ and HfV_2 are not available for a direct comparison with our calculations, we can see from Table III that the calculated cohesive energy is indeed higher for NbCr2 which has the higher melting temperature. The cohesive energies of other intermetallic compounds that have simpler crystal structures, such as $B2$ or $L1_2$, are smaller than those we calculated for $C15$ $NbCr_2$ (6.08 eV/atom) and $C15$ HfV_2 (5.69 eV/atom);

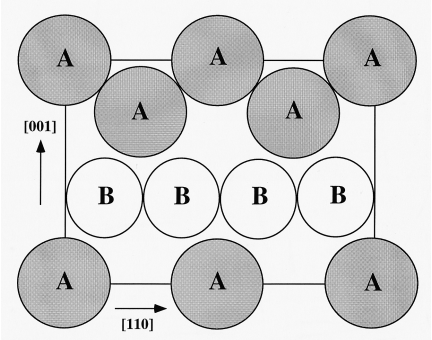

FIG. 6. The positions of the atoms on the (110) plane of the $C15$ structure for a material AB_2.

for example, the cohesive energies for $B2$ NiAl and $L1_2$ Ni_3Al are 4.52 and 4.57 eV/atom, respectively.[38]

Also listed in Table III are the calculated heats of formation, ΔH, for both compounds. The heat of formation is the difference between the total energy of the compound and the sum of the total energies of the constituents in proportion to the composition. For a Laves phase this energy per atom is given by $\Delta H=(E_{AB_2}-E_A-2E_B)/3$. We carried out full-potential LMTO calculations to obtain the elemental total energies as noted in Sec. III. From Table III we see that the heat of formation of $C15$ HfV_2 is -15.7 meV/atom. There are no experimental values cited for HfV_2. The heat of formation of $C15$ $NbCr_2$ is found to be -72.9 meV/atom. There is no direct measurement of the heat of formation of $NbCr_2$; however there is a calculated number, -73 meV/atom at 298 K, based on other thermodynamical data.[39] For the sake of completeness, we should also mention the semi-empirical method of deBoer *et al.*[40] which predicts $\Delta H = -31$ meV/atom for HfV_2 and -104 meV/atom for $NbCr_2$.

B. Elastic properties

Elastic properties of a solid are important because they relate to various fundamental solid state phenomena such as mechanical properties, equations of state, and phonon spectra. Elastic properties are also linked thermodynamically to specific heat, thermal expansion, Debye temperature, and Gruneisen parameter. Most importantly, knowledge of elastic constants is essential for many practical applications related to the mechanical properties of a solid: load-deflection behavior, thermoelastic stress, internal strain (residual stress), sound velocity, dislocation core structure, and fracture toughness.

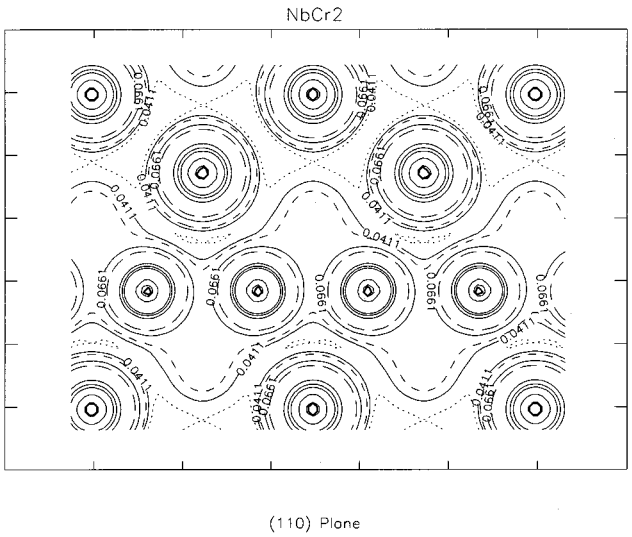

FIG. 7. Charge density contour plot in the (110) plane of $C15$ $NbCr_2$.

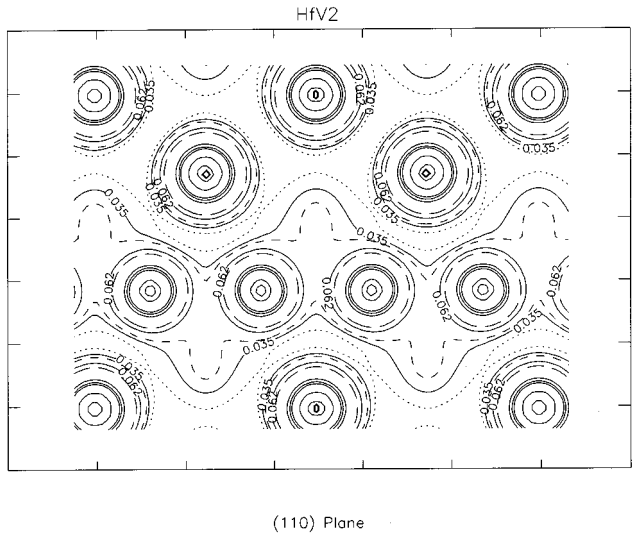

FIG. 8. Charge density contour plot in the (110) plane of $C15$ HfV_2.

Room temperature elastic moduli of polycrystalline $C15$ $NbCr_2$ and HfV_2 were measured by the resonant ultrasound spectroscopy (RUS) technique[26,41] and the bulk moduli, for example, were found to be 229.4 GPa and 104 GPa, respectively. These experimental values compare fairly well with our calculated values listed in Table I. Local density approximation based methods usually overestimate the bonding, resulting in a smaller theoretical equilibrium volume compared to the experimental one. The bulk modulus is computed as the second volume derivative of the total energy. Since the volume at which the total energy is minimum is somewhat off from the experimental volume, usually the bulk modulus computed at the theoretical volume is larger than the experimentally measured value. If, on the other hand, the bulk modulus is computed at the experimental volume, then due to the fact that total energy vs volume curve does not pass through a minimum at that volume, and that the curvature is

TABLE III. Calculated values of cohesive energies, heats of formation, and the experimentally measured melting temperatures of the Laves phases $NbCr_2$ and HfV_2.

Material	Cohesive energy per atom (eV)	Heat of formation per atom (meV)	Melting temperature (°C)
$C15$ $NbCr_2$	6.08	− 72.9	1730
$C15$ HfV_2	5.69	− 15.7	1550

usually smaller at that point, the result is a smaller modulus. Therefore, usually, the theoretically computed values sandwich the experimentally measured value. This is the case for $NbCr_2$. A second reason for the discrepancy is the effect of temperature. The experimental value was determined at room temperature, whereas the calculation is valid at 0 K, and the bulk modulus of $C15$ $NbCr_2$, as is the case for most materials, has been found to decrease with increasing temperature.[26] For HfV_2, the experimental number, 104 GPa, is slightly smaller than the calculated value at the experimental volume, 107 GPa. However, it is highly likely that the sample on which the measurement was made contained some microvoids (so the sample did not reach the theoretical density), and hence gave a smaller experimental value.[42]

A higher bulk modulus value implies a harder material, and both theory and experiment give the consistent trend that $NbCr_2$ is harder than HfV_2.

C. Phase stability: *C*15 versus *C*14

Generally speaking, among the three Laves phases ($C15$, $C14$, and $C36$), $C15$ is the low-temperature phase except for some special systems, e.g., $ScFe_2$, for which the structure sequence is, from high to low-temperatures, $C36$, $C15$, and $C14$.[34] Although an analysis of structural stability at finite temperatures requires comparing free energies, due to the fact that at 0 K the entropy contribution is zero, the total ground-state energies we have computed will be used to discuss the stability of the Laves phases at 0 K.

Experimentally, it is found that the $C15$ $NbCr_2$ phase is the stable phase at low-temperatures, $T<1585\,^{\circ}\mathrm{C}$, and the $C14$ phase is stable at higher-temperatures, $1585\,^{\circ}\mathrm{C}<T<1730^{\circ}\mathrm{C}$.[9] From Fig. 2, we see that our calculation correctly places the $C15$ phase below the $C14$ phase for all the unit cell volumes considered. From Tables I and II, we calculate the energy difference between the two phases as 20 meV/atom, which corresponds to ~ 231 K. This is reasonable because the $C14$ structure can be derived from $C15$ by {111} stacking faults in the $\alpha c \beta$ type of sandwich. Furthermore, from the energy difference between the $C15$ and $C14$ phases, the stacking fault energy γ in the $\alpha c \beta$ type of sandwich can be determined as 90 $\mathrm{mJ/m^2}$ which is in good agreement with experiment.[43] The {111} stacking fault energies of most fcc metals are also of the same order of magnitude,[44] for example, $\gamma_{\mathrm{Au}}= 32\ \mathrm{mJ/m^2}$, $\gamma_{\mathrm{Cu}}= 45\ \mathrm{mJ/m^2}$, $\gamma_{\mathrm{Ni}}= 128\ \mathrm{mJ/m^2}$, and $\gamma_{\mathrm{Al}}= 166\ \mathrm{mJ/m^2}$. However, this stacking fault energy is low compared to those of other intermetallic compounds,[45] which typically vary between 100 and 800 $\mathrm{mJ/m^2}$. In fact, in Laves phases, the only experimentally observed stacking faults are those in the $\alpha c \beta$-type of sandwich,[29] presumably due to the low stacking fault energy. On the other hand, due to the low stacking fault energy in the $\alpha c \beta$-type sandwich, synchro-shear Shockley partial dislocations may be operative in the process of plastic deformation, which is believed to be the physically plausible deformation mechanism in Laves phases.[6,10,11,46]

For the HfV_2 system, in contrast to the $NbCr_2$ case, we find that the $C14$ structure has a lower total energy than the $C15$ structure; cf. Fig. 3. This means that, for the HfV_2 system, $C15$ should be the high-temperature phase and at low-temperatures $C15$ should be unstable. Indeed, the $C15$ structure is thermally stable until the melting temperature of HfV_2, 1550 °C;[34] and it has been shown experimentally that at 115 K $C15$ HfV_2 undergoes a structural transformation.[41,47–49] However, the crystal structure of this low-temperature HfV_2 phase is not the $C14$ phase and its nature is still being investigated. A total-energy calculation for this new structure may yield a total energy lower than that for the $C14$ phase. The question of whether a large vibrational entropy that may be associated with the unusually low shear and Young's moduli in $C15$ HfV_2 (Refs. 41, 42, 25, and 26) and can stabilize the $C15$ structure relative to the $C14$ structure above 115 K will be explored further in our future studies.

D. Bonding characteristics

In solids, Poisson's ratio ν is bounded by 0.0 and 0.5, most of the measured values falling in the range 0.28–0.42. Poisson's ratio provides more information about the characteristics of the interatomic forces than any of the other elastic coefficients.[51] It has been shown that central-force-type models work very well for materials with $\nu \geqslant 0.25$.[50] Most solids belong to this category. The central-force-type models are not adequate for the description of materials for which $\nu < 0.25$. However, for $C15$ $NbCr_2$ and HfV_2, Poisson's ratios are determined to be 0.34 and 0.38, respectively.[26] These high ν values suggest that the interatomic forces in these $C15$ Laves phase compounds are not strongly directional. Charge density contour plots for $C15$ structures are shown in Fig. 7 for $NbCr_2$ and in Fig. 8 for HfV_2. The contour plots are very similar for both compounds, and do not indicate strong directionality in the bonding. Although this is a qualitative observation, it correlates well with the results of Poisson's ratio measurements.[25,26,52] Based on this agreement, it may be worthwhile to generate empirical interatomic potentials of central-force type for $C15$ $NbCr_2$ and HfV_2, which can be used to simulate the atomistic structures of a variety of defects in these materials.

VI. CONCLUSION

First-principles electronic structure calculations based on the local density approximation have been used to study various ground-state properties of the early transition metal Laves phase compounds $NbCr_2$ and HfV_2. Our results for the equilibrium unit cell volumes and bulk moduli are in good agreement with experimental results, and in general the errors are within the typical error range of LDA-based methods. From the total-energy calculations we find that $C15$ $NbCr_2$ has a lower total energy than the $C14$ structure, in agreement with experiment. For the HfV_2 system, our calculations show that the $C14$ structure has a lower total energy than the $C15$ structure, indicating that the $C15$ phase observed at high-temperatures should become unstable at lower-temperatures. A recent experimental study indeed

finds a structural transformation at $T<115$ K from $C15$ to a yet-undetermined structure.

The cohesive energy difference between $C15$ and $C14$ phases is very small, 20 meV/atom for both compounds. This implies a low stacking fault energy in the $\alpha c \beta$-type sandwiches. Hence, the deformability of this type of sandwich, via synchro-shear, is physically reasonable.

The interatomic bonding in both compounds is found to be only weakly directional, which suggests that central-force-type interatomic potentials may be suitable for some atomistic calculations.

ACKNOWLEDGMENTS

This research was performed under the auspices of the U.S. Department of Energy, Office of Basic Energy Sciences. Computer time was provided by the Energy Research/ Scientific Computing Section of the Department of Energy at the National Energy Research Supercomputer Center (NERSC).

[1] D. P. Pope and C. T. Liu, in *Superalloys, Supercomposites and Superceramics*, edited by J. K. Tien and T. Caulfield (Academic Press, New York, 1989).

[2] For a collection of recent work on aluminides, see, for example, *High Temperature Structural Intermetallic Alloys-VI*, MRS Symposia Proceedings No. 364, edited by J. Horton, I. Baker, S. Hanada, and R. D. Noebe (Materials Research Society, Pittsburgh, 1995).

[3] D. P. Pope and F. Chu, in *Structural Intermetallics*, edited by R. Darolia *et al.* (TMS Publications, Warrendale, PA, 1993).

[4] T. E. Mitchell, R. G. Castro, J. J. Petrovic, S. A. Maloy, O. Unal, and M. M. Chadwick, Mater. Sci. Eng. A **155**, 241 (1992).

[5] *Intermetallic Compounds*, edited by J. H. Westbrook (John Wiley & Sons, Inc., New York, 1967).

[6] F. Chu and D. P. Pope, Mater. Sci Eng. A **170**, 39 (1993).

[7] R. L. Fleischer, J. Mater. Sci. **22**, 2281 (1987).

[8] M. Takeyama and C. T. Liu, Mater. Sci. Eng. A **132**, 61 (1991).

[9] D. J. Thoma and J. H. Perepezko, Mater. Sci. Eng. A **156**, 97 (1992).

[10] J. D. Livingston and E. L. Hall, J. Mater. Res. **5**, 5 (1990).

[11] K. S. Kumar and P. M. Hazzledine, in *High Temperature Structural Intermetallic Alloys-VI*, MRS Symposia Proceedings No. 364, edited by J. Horton, I. Baker, S. Hanada, and R. D. Noebe (Materials Research Society, Pittsburgh, 1995), p. 1383.

[12] Y. Liu, S. M. Allen, and J. D. Livingston, in *High Temperature Ordered Intermetallic Alloys-V*, edited by I. Baker, R. Dorolia, J. D. Whittenberger, and M. H. Yoo, MRS Symposia Proceedings No. 288 (Materials Research Society, Pittsburg, PA, 1993), p. 203.

[13] K. Chen, S. M. Allen, and J. D. Livingston, in *High Temperature Ordered Intermetallic Alloys-V* (Ref. 12), p. 373.

[14] T. Jarlborg and A. J. Freeman, Phys. Rev. B **22**, 2332 (1980).

[15] P. Rennert and M. Taut, Phys. Status Solidi **41**, 703 (1970).

[16] D. L. Johnson, Phys. Rev. B **9**, 2273 (1974).

[17] A. C. Switendick, in *Proceedings of the 10th Rare Earth Research Conference*, edited by C. J. Kevane and T. Moeller (Carefree, Arizona, 1973), p. 235.

[18] K. Terao and M. Shimizu, Phys. Status Solidi B **139**, 485 (1987).

[19] S. Asano and S. Ishida, J. Phys. F **18**, 501 (1988).

[20] P. Rennert and A. M. Radwan, Phys. Status Solidi B **79**, 167 (1977).

[21] R. Haydock and R. L. Johannes, J. Phys. F **5**, 2055 (1975).

[22] Y. Ohta and D. G. Pettifor, J. Phys. Condens. Matter **2**, 8189 (1990).

[23] R. L. Johnston and R. Hoffman, Z. Anorg. Allg. Chem. **616**, 105 (1992).

[24] M. Sluiter and P. E. A. Turchi, Phys. Rev. B **43**, 12 251 (1991).

[25] F. Chu, M. Sob, R. Siegl, T. E. Mitchell, D. P. Pope, and S. P. Chen, Philos. Mag. B **70**, 881 (1994).

[26] F. Chu, D. J. Thoma, Y. He, T. E. Mitchell, S. P. Chen, and J. Perepezko, p. 1089; F. Chu, T. E. Mitchell, S. P. Chen, M. Sob, R. Siegl, and D. P. Pope, in *High Temperature Structural Intermetallic Alloys-VI*, MRS Symposia Proceedings No. 364, edited by J. Horton, I. Baker, S, Hanada, and R. D. Noebe (Materials Research Society, Pittsburgh, 1995), p. 1389.

[27] See, in addition to Refs. 5 and 24 cited above, W. B. Pearson, *The Crystal Chemistry and Physics of Metals and Alloys* (John Wiley & Sons, Inc., New York, 1972); A. K. Sinha, in *Progress in Mater. Science*, Vol. 15, edited by B. Chalmers, J. W. Christian, and T. B. Massalski (Pergamon Press, New York, 1972).

[28] James B. Friauf, Phys. Rev. **29**, 34 (1927).

[29] C. W. Allen, P. Delvavignette, and S. Amelinckx, Phys. Status Solidi A **9**, 237 (1972).

[30] J. M. Wills (unpublished); J. M. Wills and B. R. Cooper, Phys. Rev. B **36**, 3809 (1987); D. L. Price and B. R. Cooper, *ibid.* **39**, 4945 (1989).

[31] L. Hedin and B. I. Lundqvist, J. Phys. C **4**, 2064 (1971).

[32] V. L. Moruzzi, J. F. Janak, and A. R. Williams, *Calculated Electronic Properties of Metals* (Pergamon Press, New York, 1978).

[33] S. Froyen, Phys. Rev. B **39**, 3168 (1989).

[34] *Binary Phase Diagram*, edited by T. B. Massalski (ASM, Pittsburgh, PA, 1982).

[35] J. M. Wills (unpublished).

[36] F. D. Murnaghan, Proc. Natl. Acad. Sci. USA **30**, 244 (1944); F. Birch, J. Geophys. Res. **57**, 227 (1952).

[37] S. P. Chen, D. J. Srolovitz, and A. F. Voter, J. Mater. Res. **4**, 62 (1989); S. P. Chen *et al.*, *ibid.* **5**, 955 (1990).

[38] R. Hultgren, R. L. Orr, P. D. Anderson, and K. K. Kelley, *Selected Value of the Thermodynamic Properties of Metals and Binary Alloys* (John Wiley, New York, 1973), p. 191.

[39] J. F. Martin, Franz Müller, and O. Kubaschewski, Trans. Faraday Soc. **66**, 1065 (1970).

[40] F. R. deBoer, R. Boom, W. C. M. Mattens, A. R. Miedema, and A. K. Niessen, *Cohesion in Metals* (North-Holland, Amsterdam, 1989). In addition to the description of their model and an overview of cohesion in transition metal alloys, they also present a collection of thermodynamical data on numerous alloys. See p. 175 or 392 for $NbCr_2$ and p. 150 or 526 for HfV_2.

[41] A. S. Balankin, Yu F. Bychkov, and Ye I. Yakovlev, Phys. Met. Metall. **56**, 119 (1983).

[42] F. Chu, M. Lei, A. Migliori, S. P. Chen, and T. E. Mitchel, Philos. Mag. B **70**, 867 (1994).

[43] F. Chu, A. H. Ormeci, T. E. Mitchell, J. M. Wills, D. J. Thoma,

R. C. Albers, and S. P. Chen, Philos. Mag. Lett. **72**, 147 (1995).
[44] J. P. Hirth and J. Lothe, *Theory of Dislocations* (John Wiley & Sons, New York, 1982).
[45] C. L. Fu, J. Mater. Res. **5**, 971 (1990); C. L. Fu and M. H. Yoo, Mater. Chem. Phys. **32**, 25 (1992).
[46] P. M. Hazzledine and P. Pirouz, Scr. Met. Mater. **28**, 1277 (1993).
[47] T. R. Finlayson, E. J. Lanston, M. A. Simpson, E. E. Gibbs, and T. F. Smith, J. Phys. F **8**, 2269 (1978).
[48] J. W. Hafstrom, G. S. Knapp, and A. T. Aldred, Phys. Rev. B **17**, 2892 (1978).
[49] F. Chu, Ph.D. thesis, University of Pennsylvania, Philadelphia, 1993.
[50] H. M. Ledbetter, in *Materials at Low Temperatures*, edited by R. P. Reed and A. F. Clark (American Society for Metals, Metals Park, OH, 1983).
[51] W. Koster and H. Franz, Metall. Rev. **6**, 1 (1961).
[52] F. Chu (unpublished).